Eleventh U.S. National Conference on Earthquake Engineering
Integrating Science, Engineering & Policy
June 25-29, 2018
Los Angeles, California

INELASTIC TIME HISTORY RESPONSE OF LUMPED PARAMETER WALL AND DIAPHRAGM BUILDING

A.W. Fischer[1] and B.W. Schafer[2]

ABSTRACT

The objectives of this paper are to investigate the time history response of buildings across a wide range of wall and diaphragm periods, where inelastic behavior in both the walls and diaphragms is possible, and compare this behavior with current design assumptions. Design specifications such as ASCE7-16 are beginning to explicitly recognize and account for inelasticity in both the vertical (walls) and horizontal (diaphragms) lateral force resisting systems (vLFRS and hLFRS) during earthquakes. Newly developed diaphragm provisions now appearing as an alternate method in ASCE7 explicitly include inelasticity. Additionally, FEMA work has proposed new design procedures for rigid wall flexible diaphragm buildings that depart from the traditional view where all inelasticity is accounted for in the designated vLFRS. Left unanswered in these new approaches is how stiffness, mass, and ductility of the vertical and horizontal lateral force resisting systems interact – and whether inelasticity in the two systems can be considered independently and utilize their own seismic response modification coefficients (i.e. R for vLFRS and R_s for hLFRS). In the models employed herein each building story is approximated as three lumped masses, representing the walls and a diaphragm, connected through springs. The period of walls and diaphragms is varied, resulting in a large number of different potential building response. Vibration analysis and nonlinear time history analyses are performed on the models. Employing the FEMA P695 suite of 22 earthquakes, the average forces and ductility demands in walls and diaphragms are studied. The elastic interaction between walls and diaphragms is found to be greatest when the periods are similar; and this relation is likewise found in the inelastic studies. The building demands, when the walls are inelastic and the diaphragms are elastic, depend on the mass distribution, but generally follow the change of demand in the inelastic walls. More complex cases are studied and interactions, when either system is inelastic, are complex and summaries of base shear, wall/floor ductility demands, and equivalent lateral forces

[1]Graduate Student, Dept. of Civil Engineering, Johns Hopkins University, Baltimore, MD USA, Winther@jhu.edu
[2]Professor, Dept. of Civil Engineering, Johns Hopkins University, Baltimore, MD USA, Schafer@jhu.edu

Lord J, Wright R. Template to illustrate paper format for the 11NCEE. *Proceedings of the 11th National Conference in Earthquake Engineering*, Earthquake Engineering Research Institute, Los Angeles, CA. 2018.

will demonstrate the results. This study has illuminated the interactions between walls and diaphragm in seismic analysis, and provided a better understanding for structural elements influence on each other during seismic loading. This work is part of a larger Steel Diaphragm Innovation Initiative and aims to better understand the role of inelastic diaphragm response on the behavior of steel buildings. Future work investigating more specific building archetypes and nonlinear full building models is underway.

Eleventh U.S. National Conference on Earthquake Engineering
Integrating Science, Engineering & Policy
June 25-29, 2018
Los Angeles, California

Inelastic Time History Response of Lumped Parameter Wall and Diaphragm Building

A.W. Fischer[1] and B.W. Schafer[2]

ABSTRACT

The objectives of this paper are to investigate the time history response of buildings across a wide range of wall and diaphragm periods, where inelastic behavior in both the walls and diaphragms is possible, and compare this behavior with current design assumptions. Design specifications such as ASCE7-16 are beginning to explicitly recognize and account for inelasticity in both the vertical (walls) and horizontal (diaphragms) lateral force resisting systems (vLFRS and hLFRS) during earthquakes. Newly developed diaphragm provisions now appearing as an alternate method in ASCE7 explicitly include inelasticity. Additionally, FEMA work has proposed new design procedures for rigid wall flexible diaphragm buildings that depart from the traditional view where all inelasticity is accounted for in the designated vLFRS. Left unanswered in these new approaches is how stiffness, mass, and ductility of the vertical and horizontal lateral force resisting systems interact – and whether inelasticity in the two systems can be considered independently and utilize their own seismic response modification coefficients (i.e. R for vLFRS and R_s for hLFRS). In the models employed herein each building story is approximated as three lumped masses, representing the walls and a diaphragm, connected through springs. The period of walls and diaphragms is varied, resulting in a large number of different potential building response. Vibration analysis and nonlinear time history analyses are performed on the models. Employing the FEMA P695 suite of 22 earthquakes, the average forces and ductility demands in walls and diaphragms are studied. The elastic interaction between walls and diaphragms is found to be greatest when the periods are similar; and this relation is likewise found in the inelastic studies. The building demands, when the walls are inelastic and the diaphragms are elastic, depend on the mass distribution, but generally follow the change of demand in the inelastic walls. More complex cases are studied and interactions, when either system is inelastic, are complex and summaries of base shear, wall/floor ductility demands, and equivalent lateral forces will demonstrate the results. This study has illuminated the interactions between walls and diaphragm in seismic analysis, and provided a better understanding for structural elements influence on each other during seismic loading. This work is part of a larger Steel Diaphragm Innovation Initiative and aims to better understand the role of inelastic diaphragm response on the behavior of steel buildings. Future work investigating more specific building archetypes and nonlinear full building models is underway.

[1]Graduate Student, Dept. of Civil Engineering, Johns Hopkins University, Baltimore, MD, USA, Winther@jhu.edu
[2]Professor, Dept. of Civil Engineering, Johns Hopkins University, Baltimore, MD, USA, Schafer@jhu.edu

Lord J, Wright R. Template to illustrate paper format for the 11NCEE. *Proceedings of the 11th National Conference in Earthquake Engineering*, Earthquake Engineering Research Institute, Los Angeles, CA. 2018.

Introduction

Simplified models have an important role in the development of earthquake engineering. Inelastic equivalent single degree of freedom models provide the under-pinning for the reduced (by R) pseudo spectral acceleration response spectra that are at the core of modern earthquake engineering. However, single degree of freedom models conceptualize only one system undergoing inelasticity, to understand how horizontal systems may impact vertical systems at least one additional degree of freedom is required. A simple mass-spring single-story building model that provides for the diaphragm (subscript d) and walls (subscript h) degrees of freedom was created as depicted in Figure 1.

The work here provides an extensive parametric study of single story building time history responses, and elucidates the interactions between the vertical structure (walls) and horizontal structure (diaphragm). The study included different yielding levels for both walls and diaphragms.

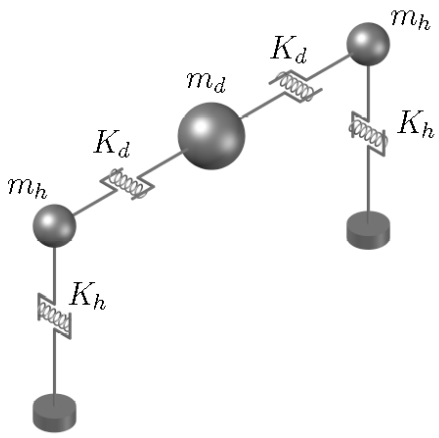

Figure 1. Mass spring model of a single-story building used for the parametric study of wall-diaphragm interactions.

Methodology

In the developed model a single-story building with perimeter frames is represented by three lumped masses and connecting springs. For lateral loads, only displacements perpendicular to the model frame are considered, leading to a 3 degree of freedom model of a single story, as shown in Figure 1. The lumped masses are defined from a mass ratio and from the total mass of the floor:

$$m_d = \alpha_m \, m \tag{1}$$

$$m_h = \frac{(1-\alpha_m)}{2} \, m \tag{2}$$

The spring stiffness are defined from the periods of the vertical and horizontal structure. Where, T_h is the first eigen period of the structure with a rigid diaphragm, T_d is the period of the structure when the walls are rigid, i.e. the period of the isolated floor system. The stiffness is therefore:

$$K_d = 2\left(\frac{\pi}{T_d}\right)^2 m_d \tag{3}$$

$$K_h = 2\left(\frac{\pi}{T_h}\right)^2 m \tag{4}$$

The inelastic behavior of the structure is assumed to be elastic perfectly plastic for both the walls and diaphragm springs. The yielding forces/displacements are defined from the elastic time history response, as the maximum force in the wall or diaphragm at the maximum considered earthquake (MCE) level divided by the response modification coefficient R_d or R_{sd} for vertical or horizontal structure, respectively.

$$V_{yh} = \frac{V_h^{mce}}{R_d} \tag{5}$$

$$V_{yd} = \frac{V_d^{mce}}{R_{sd}} \tag{6}$$

The response modification coefficients used in this study are listed in Table 1, but originate from Table 12.2-1 and Table 12.10-1 in ASCE-7 16. As indicated in Eq. (5) and (6) R_d and R_{sd} are the "ductility" portion of the response modification coefficient. For the vertical structure, a large number of members and associate response modifications factors are provided in ASCE-7 16, from this list four values are selected to represent typical structural elements in the study. While for the horizontal structure, only a few structural members and associated response factors are provided in the alternative diaphragm design of ASCE-7 16, therefore engineering judgement is used to estimate appropriate values for diaphragm overstrength factors.

Table 1. Response modification factors selected for this study. Response factors for the vertical structural system are selected from Table 12.2-1 in ASCE-7 16. For the horizontal system, resistance factors are selected from Table 12.10-1 in ASCE-7 16 and from engineering judgement.

	Elastic	**OCBF[1]**	**SMF[2] & BRB[3]**			**Elastic**	**Precast RDO[4]**	**Steel 1**	**Wood**
R[5]	1	4	3	8	R_s[6]	1	1.4	2.2	3
Ω_0	1	2	1	1.6	R_{so}	1	1	1.1	1.2
$\boldsymbol{R_d}$	**1.0**	**2.0**	**3.0**	**5.0**	$\boldsymbol{R_{sd}}$	**1**	**1.4**	**2.0**	**5**

[1] Ordinary concentrically braced frames, [2] Special moment frames,
[3] Buckling-restrained braced frames, [4] Precast concrete diaphragm reduced design option,
[5] $R = R_d R_o, R_o \cong \Omega_o$ [6] $R_s = R_{sd} R_{so}$

For the parametric studies herein, each analysis of each structure starts with an elastic time history analysis of each earthquake, resulting in a scale factor (for the desired MCE level), values for yielding forces/displacements in both walls and diaphragm, and results from the analysis. This is followed by inelastic time history analysis of the same models, now scaled to the MCE level for the elastic structure, but with inelastic material behavior. Additionally, the models in the time history analysis employ 5% Rayleigh damping in the first two vibration modes of the model. The

model is subjected to the 22 far-field earthquakes listed in FEMA P695.

Two different structural layouts are considered: $\alpha_m = [0.2, 0.9]$, representing the mass distribution one finds in a rigid wall flexible diaphragm building and in a traditional building with heavy (and typically stiff) diaphragms, respectively. Additionally, a number of different vertical periods are selected in the range: $T_h \epsilon [0.1, 2.0] s$ and a small number of ratios between horizontal and vertical periods are likewise studied: $T_d/T_h \epsilon [0.01, 10]$ for the time history analysis. A more extensive study is executed on the eigenvalue analysis. In the following only selected results are presented from the parametric time history study.

Results and Discussion

Through a parametric eigen analysis estimation of the natural period of the whole structure (T_b) is established. The natural period of the isolated horizontal and vertical structure are varied, additionally, the mass distribution in the structure (α_m) is also varied. Figure 2 shows the period of the model compared to the isolated wall and diaphragm periods and mass distribution. When $T_d \ll T_h$ the stiffness of the diaphragm is rigid, and the building period T_b approaches the period of the walls with a rigid floor system, i.e. T_h. When $T_d \gg T_h$ the diaphragm controls the first vibration mode and the first period of the building approaches T_d. Interestingly, at $T_d = T_h$ the walls and floor systems work together to elongate the period of the building by up to 40%.

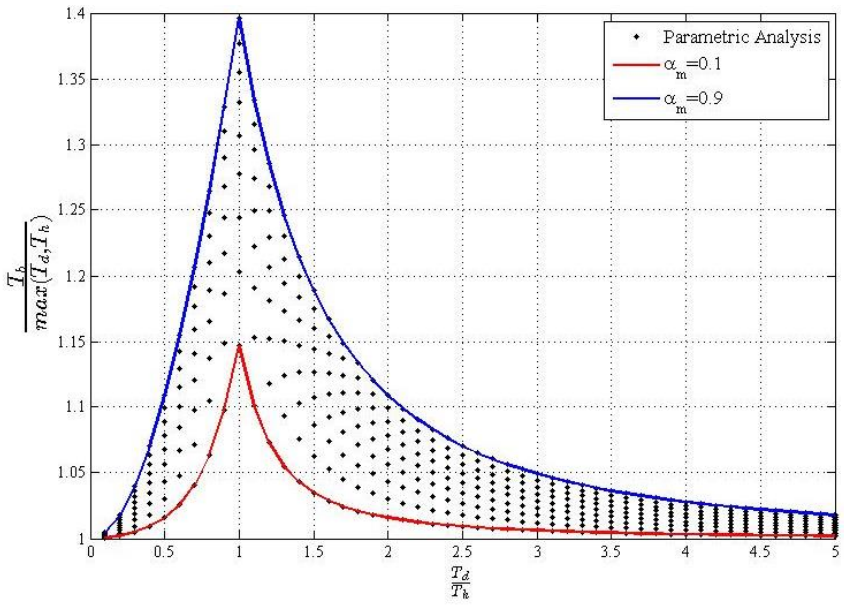

Figure 2. Building period as function of the ratio of natural period of horizontal system to period of vertical system.

The following figures summarize the mean results across the 22 earthquakes from the time history analyses as wall period and diaphragm period are varied. The figure in the top left corner represents the elastic case of both wall and diaphragm. The top row of figures is elastic diaphragm, where the R_d for the walls increases from left to right and the left column of figures represents elastic walls with yielding diaphragm (increasing R_{sd}). Only the results from the model with heavy floors ($\alpha_m = 0.9$) are presented here.

Figure 3 summarizes the forces in the walls and diaphragms for $T_d/T_h = 0.5$ (semirigid) and $T_d/T_h = 10$ (flexible). In the elastic case (top left corner) the walls are scaled to the MCE level (dotted lines) and the diaphragm forces (solid lines) are extracted and plotted against the wall forces. When R_d of the walls is increasing (lower yield force) the wall forces still follow the MCE curve, but as a fraction of the value (as expected), and with the yielding walls, the diaphragm forces are driven down to forces about the same size as the walls; however, in some cases the diaphragm forces can exceed the wall forces. For the stiffer diaphragms the diaphragm forces exceed the wall forces for any stiffness of the walls, whereas the more flexible diaphragm only exceeds the wall forces for the stiffer walls.

The left column of Figures 3-4 represents elastic walls with yielding diaphragms, and it may be observed that the stiffer diaphragms cause the wall forces to decrease as R_{sd} increases, while flexible diaphragms cause the forces in the walls to go up to a force level equal to $F_a\, S_s\, m$ and decreases for increasing wall period. When both walls and diaphragm are yielding, the forces are driven down by both the yielding walls and to a lesser extent the yielding diaphragm.

Figure 4 shows the diaphragm forces, normalized with maximum spectral acceleration (MCE level) times the mass of the diaphragm and with an x-axis equal to the ratio T_d/T_h. The top left corner presents the elastic case, and the left column is inelastic diaphragms with elastic walls, with the same curves in all the figures, just with a fraction of the values. The top row is the elastic diaphragm with an increasing wall R_d factor, here the diaphragm forces are driven down to about 30% of the elastic case for the case with $R_d = 5$.

The two horizontal lines in Figure 5 indicate the upper and lower bound for conventional diaphragm forces according to Section 12.10 in ASCE-7 16 (i.e. $0.2\, m_d S_{MS}$ and $0.4\ m_d S_{MS}$). Taken independently, wall $R_d \geq 3$ will reduce the diaphragm forces to the conventional range; or diaphragm $R_{sd} \geq 2.5$ is also adequate. Considering both yielding in the wall and diaphragm $R_d \geq 3$ and $R_{sd} \geq 2$ reduces the predicted diaphragm demand to conventional values. Thus, this model suggest that traditional diaphragm design is conservative as long as inelasticity in the walls and/or diaphragms meet these target levels – and may even be overly conservative if greater ductility is provided. However, if inelasticity is not present or limited, diaphragm demands may easily exceed conventional limits.

Figure 5 illustrates the ductility demand in the walls and diaphragm as the response factors (R_d and R_{sd}) and stiffness of walls and diaphragm are varied. Note, the inelastic deformations are mainly caused by the diaphragm when $R_d < R_{sd}$, and by the walls when $R_d > R_{sd}$. Furthermore, the ductility demands radically increase for $T_d/T_h \to 0$ (stiff diaphragm) when $R_d < R_{sd}$.

Besides the lines indicating the forces or ductility demand in the models in Figure 3-5, a number of colored dots are also indicated. These markers represent single-story archetype buildings from FEMA P695 or from the archetype study in the Steel Diaphragm Innovation Initiative project (Torabian et al. 2017). From FEMA P695 a single concrete building is estimated indicated by the blue dots in the figures, while from SDII, nine steel archetype buildings are estimated and marked with red dots. The steel buildings have stiffer walls than the concrete building, but more flexible diaphragms. Estimated values for the single-story buildings are listed in the Appendix.

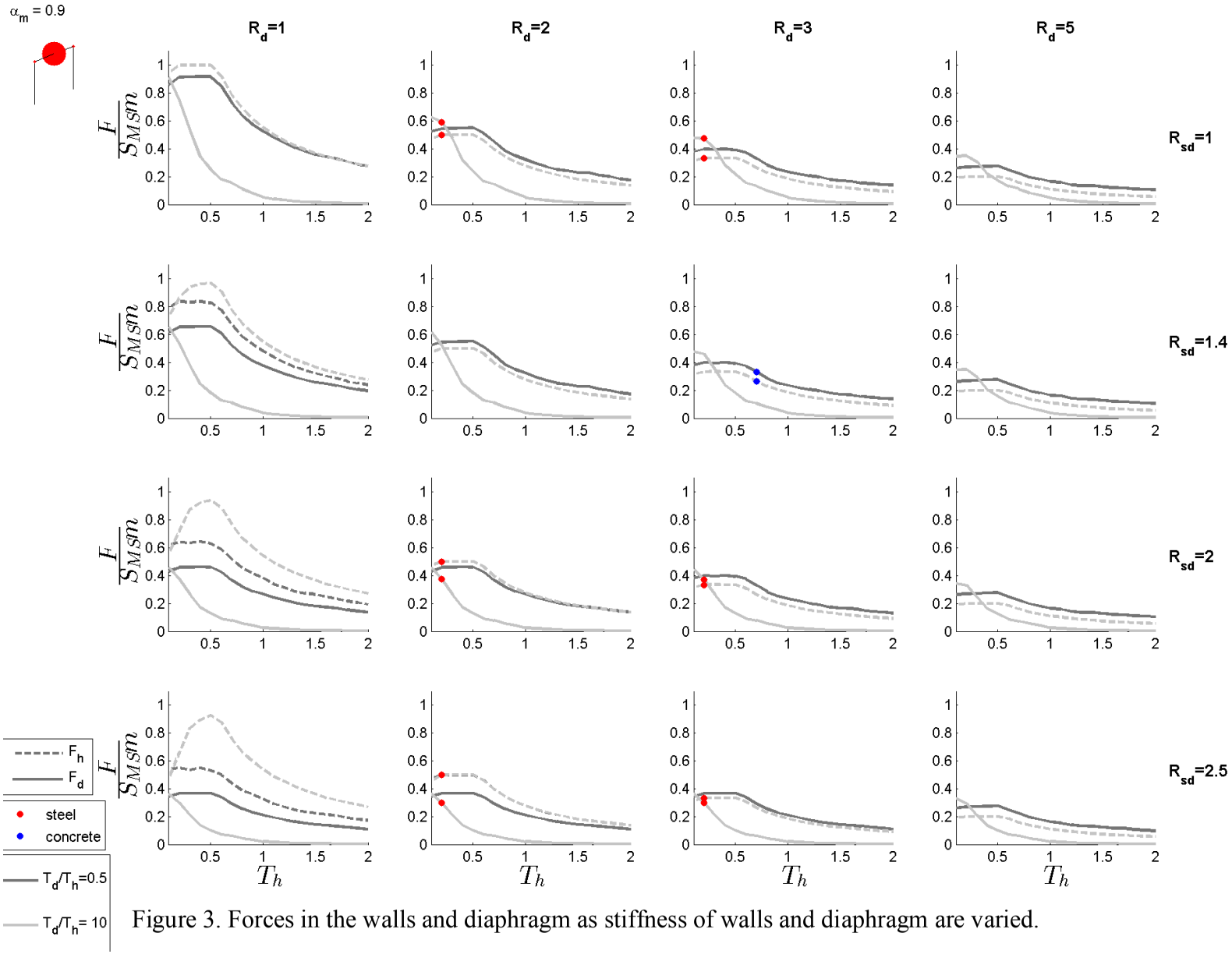

Figure 3. Forces in the walls and diaphragm as stiffness of walls and diaphragm are varied.

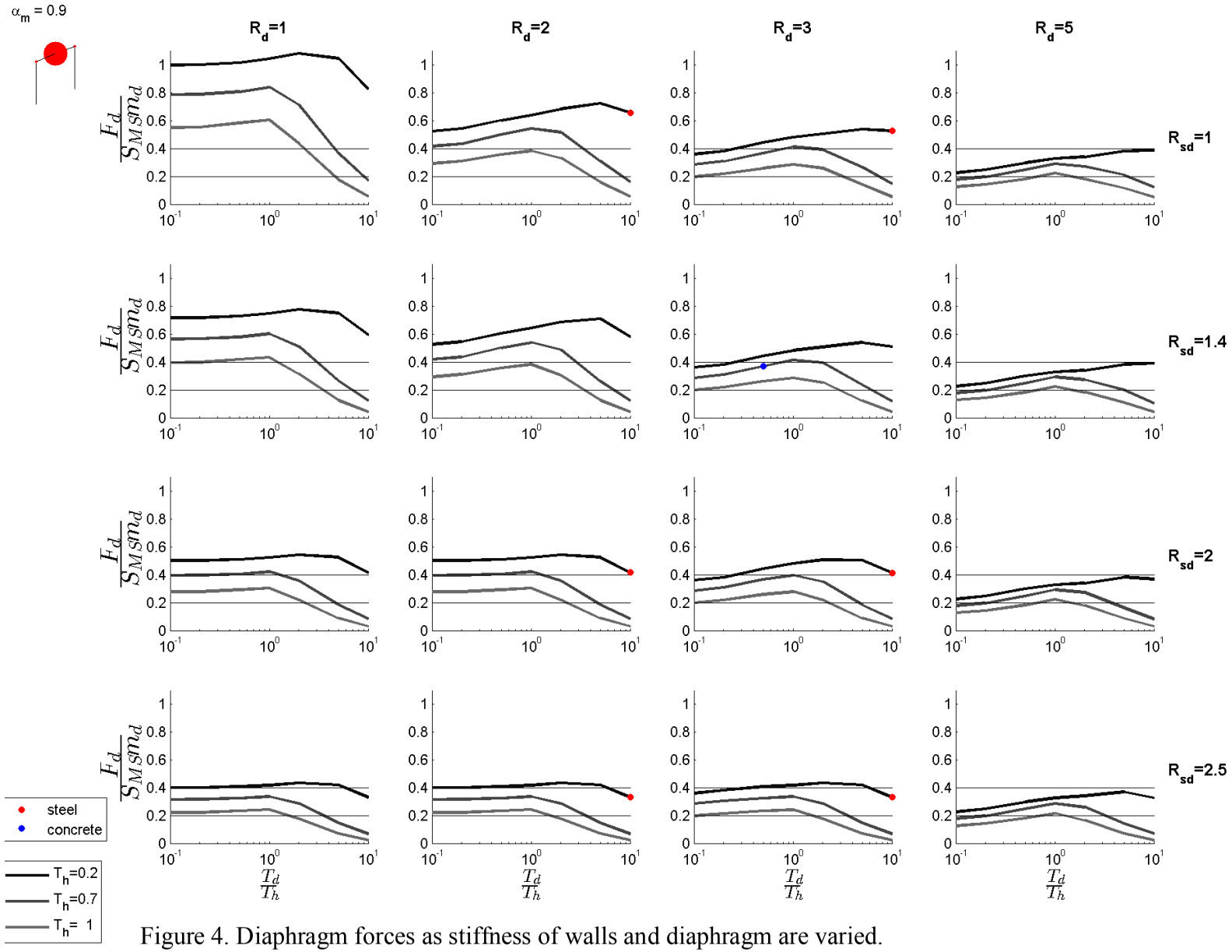

Figure 4. Diaphragm forces as stiffness of walls and diaphragm are varied.

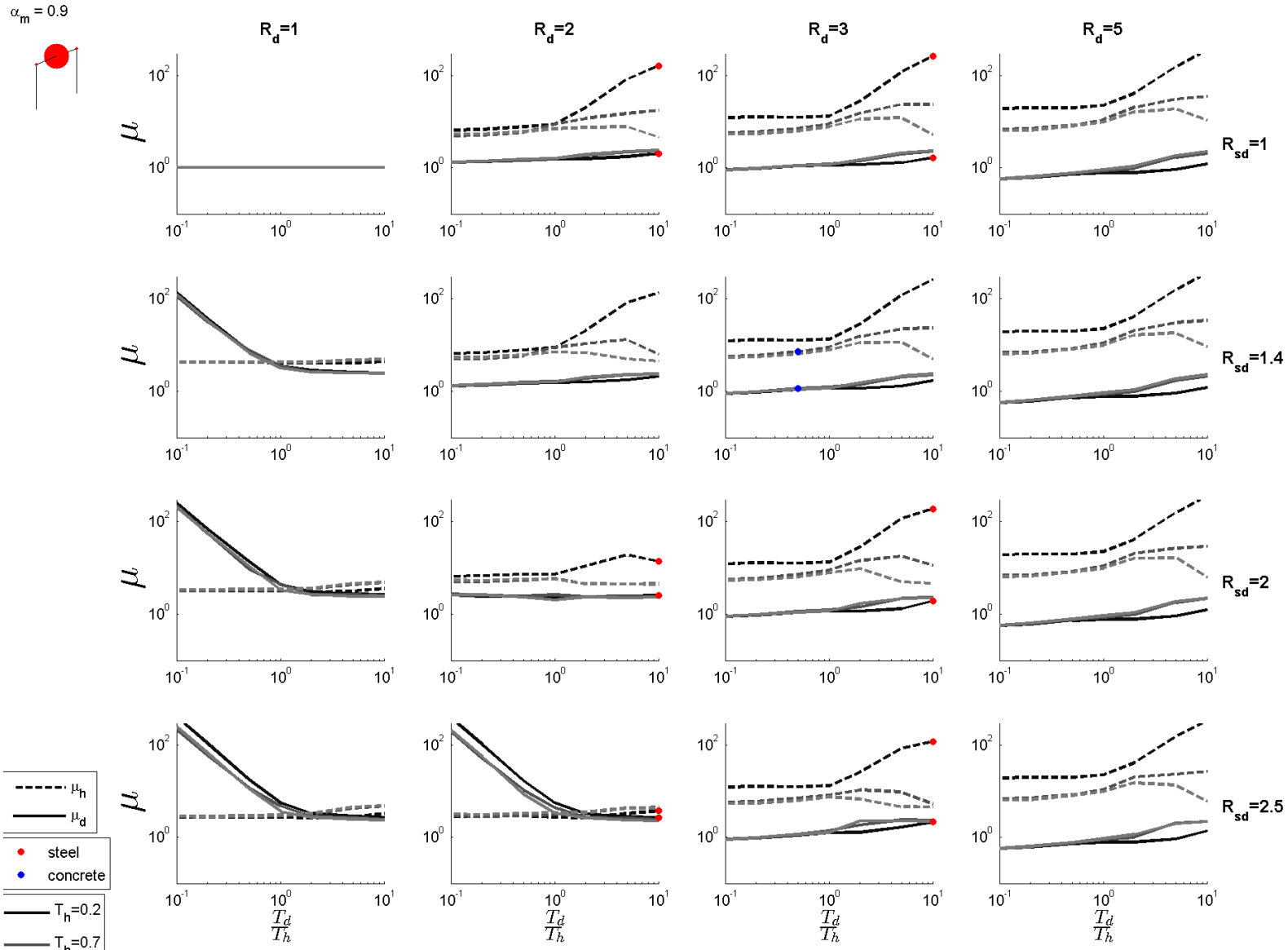

Figure 5. Ductility demand in the model as stiffness of walls and diaphragm are varied.

Conclusions

An extended parametric analysis has been performed on the nonlinear time history performance of a single-story building model. The model includes lumped masses and different stiffness and yielding parameters for its two walls and the connecting diaphragm. The parametric studies consider the period of vibration of the walls, the period of vibration of the diaphragm, and the yielding force levels for the wall and diaphragm. Eigen analysis of the model indicates the elastic regimes where the wall and diaphragm interact and serve to elongate the building period. The nonlinear time history analyses show that inelasticity in the walls is more effective at lowering forces in the wall and diaphragm than inelasticity in the diaphragm, which largely only reduces diaphragm demands. It was found that the upper and lower bounds on diaphragm demands in conventional ASCE7 diaphragm design are not realized in the studied model. Further, it was found that only if $R_d \geq 3$ and $R_{sd} \geq 2$ are the conventional bounds on diaphragm design approximately appropriate and conservative. Considering the ductility demand it was found that when R_{sd} is larger than R_d, the diaphragm has the greatest ductility demand, while for larger R_d, the walls control the ductility demand. The component that yields first sees the greatest ductility demand even if the other building component also yields. The ductility demand in the diaphragm depends on the ratio between the diaphragm period to wall period, and for stiff diaphragms, the ductility demand can be significant.

Acknowledgments

The authors gratefully acknowledge the financial support of the US National Science Foundation through grant CMMI-1562821 and of industry through the Steel Diaphragm Innovation Initiative (SDII). Collaborators in the SDII project have provided the authors with assistance throughout the work on this paper, and acknowledge the ideas and contributions they have given. In addition, the authors would like to thank Dr. Shahab Torabian, for his early work, continuous assistance through the project and the drawing of the 3 DOF model used in this paper. Any opinions, findings, and conclusions or recommendations expressed in this material are those of the author(s) and do not necessarily reflect the views of the National Science Foundation or other sponsors.

Appendix

Single-story archetype buildings, estimated values for characterizing the buildings.

From	no# stories	Material	R_d	R_{sd}	α_m	T_h	T_d/T_h
FEMA P695	1	concrete	2.67	1.4	0.9	0.71	0.5
SDII Archetype	1	steel	3.20	2	0.9	0.217	10
SDII Archetype	1	steel	3.20	1	0.9	0.217	10
SDII Archetype	1	steel	3.20	3	0.9	0.217	10
SDII Archetype	1	steel	3.00	2	0.9	0.217	10
SDII Archetype	1	steel	3.00	1	0.9	0.217	10
SDII Archetype	1	steel	3.00	3	0.9	0.217	10
SDII Archetype	1	steel	1.63	2	0.9	0.217	10
SDII Archetype	1	steel	1.63	1	0.9	0.217	10
SDII Archetype	1	steel	1.63	3	0.9	0.217	10

References

1. ASCE. (2016). Minimum Design Loads for Building and Other Structures. *ASCE 7-16*. American Society of Civil Engineers.
2. FEMA. (2000, September). State of the Art Report on Systems Performace of Steel Moment Frames Subject to Eathquake Ground Shaking. *FEMA-355C*. Federal Emergency Management Agency.
3. FEMA. (2009, June). Quantification of Building Seismic Performance Factors. *FEMA-P695*. Federal Emergency Management Agency.
4. Torabian, S., Eatherton, M., Easterling, W., Hajjar, J., & Schafer, B. (2017). *SDII Building Archetype Design v1.0.* Cold-Formed Sttel Research Consortium. Retrieved from http://jhir.library.jhu.edu/handle/1774.2/40638